

## ***Ab-Initio* Calculations of Photonic Structures**

### **Academic and Research Staff**

Professor J. D. Joannopoulos  
Professor Marin Soljačić

### **Visiting Scientists and Research Affiliates**

Dr. Ivan Celanovic

### **Postdoctoral Fellows**

Dr. Jorge Bravo-Abad  
Dr. Peter Bermel  
Dr. Zheng Wang  
Dr. Aristeidis Karalis

### **Graduate Students**

Michael Ghebrebrhan  
Rafif Hamam  
Song Liang Chua  
Wenjun Qiu  
Andre Kurs  
Alejandro Rodriguez  
Bo Zhen  
Adrian Y. X. Yeng  
Jeongwon Lee  
Ognjen Ilic

### **Undergraduate Students**

David Ramirez  
Kenny Lam

### **Technical and Support Staff**

Margaret O'Meara

## **Summary**

We show theoretically how the light-confining properties of triply-resonant photonic resonators can be tailored to enable dramatic enhancements of the conversion efficiency of THz generation via nonlinear frequency down-conversion processes. Using detailed numerical calculations, we predict that this approach can be used to reduce up to three orders of magnitude the pump powers required to reach quantum-limited conversion efficiency of THz generation in conventional nonlinear optical material systems. Furthermore, we propose a realistic design readily accessible experimentally, both for fabrication and demonstration of optimal THz conversion efficiency at sub-W power levels.

**Efficient low-power terahertz generation via on-chip triply-resonant nonlinear frequency mixing****Sponsors**

National Science Foundation - DMR 0819762

Institute for Soldier Nanotechnologies - W911NF-07-D-0004

**Project Staff**

Jorge Bravo-Abad

John D. Joannopoulos

Steven G. Johnson

Peter T. Rakich

Alejandro W. Rodriguez

M. Soljačić

Achieving efficient terahertz (THz) generation using compact turn-key sources operating at room temperature and modest power levels represents one of the critical challenges that must be overcome to realize truly practical applications based on THz.<sup>1</sup> Up to now, the most efficient approaches to THz generation at room temperature — relying mainly on optical rectification schemes — require intricate phase-matching set-ups and powerful lasers.<sup>2,3</sup> Recently, different approaches to resonant enhancement of difference-frequency nonlinear coupling processes, including those involving a final frequency in the THz regime, have been proposed.<sup>4,5</sup> However, to our knowledge, none of these previous approaches as they stand now, allow reaching conversion efficiencies close to the so-called quantum-limit<sup>6</sup> in a compact device operating at room-temperature. In this letter, we present a scheme that enables enhancement of THz power generation via second-order nonlinear frequency down-conversion by up to three orders of magnitude compared to conventional non-resonant approaches. By using a combination of accurate numerical simulations and a rigorous coupled-mode theory, we show how the unique properties of photonic microresonators to confine light in subwavelength volumes for many optical periods enable the implementation of highly-efficient compact on-chip continuous-wave THz sources operating at room temperature and pumped by sub-W pulses, which could contribute to the practical realization of efficient THz sources that are turn-key and low cost.

Our approach is motivated by the following physical picture of an arbitrary cavity-enhanced second-order nonlinear difference-frequency generation process. Consider a resonant nonlinear electromagnetic (EM) cavity characterized by a certain second-order nonlinear susceptibility tensor  $\chi_{ijk}^{(2)}(\mathbf{r})$  (subindices  $\{i, j, k\}$  stand for the cartesian components  $\{x, y, z\}$ , respectively). Imagine further that the cavity is designed to confine, both spatially and temporally, the frequency difference  $\omega_T$ , but it is otherwise transparent for both the pump and idler frequencies (denoted by  $\omega_1$  and  $\omega_2$ , respectively, defined so  $\omega_T = \omega_1 - \omega_2$ ). In such a system, the temporal variation of the nonlinear polarization vector  $\mathbf{P}^{NL}(\mathbf{r}, t)$ , induced in the system by the pump and idler electric fields ( $\mathbf{E}_1(\mathbf{r}, t)$  and  $\mathbf{E}_2(\mathbf{r}, t)$ , respectively), yields a current distribution,  $\mathbf{J}_T(\mathbf{r}, t) = \partial \mathbf{P}^{NL}(\mathbf{r}, t) / \partial t$ , which emits radiation at  $\omega_T$  inside the cavity. The power radiated by  $\mathbf{J}_T(\mathbf{r}, t)$ , and, therefore, the overall efficiency of the nonlinear frequency-mixing process, is strongly enhanced as a result of the significant modification of the electromagnetic density modes induced by the cavity in the medium in which the current  $\mathbf{J}_T(\mathbf{r}, t)$  is embedded in;<sup>7</sup> much in the same way as the spontaneous emission rate of a quantum emitter is enhanced when it is placed inside a resonant cavity, the so-called Purcell enhancement.<sup>8</sup> In fact, noticing that the power radiated by  $\mathbf{J}_T(\mathbf{r}, t)$  inside the cavity is given by

$(1/2) \text{Re} \left[ \int_{V_{NL}} \mathbf{J}_T(\mathbf{r}, t) \mathbf{E}_T^*(\mathbf{r}, t) \right]$  (where  $V_{NL}$  denotes the volume of the nonlinear cavity and  $\mathbf{E}_T(\mathbf{r}, t)$

corresponds to the cavity resonant mode at  $\omega_T$ ; normalized so that  $U_T = (1/2) \int_{V_{NL}} \varepsilon_0 n_T^2 |\mathbf{E}(\mathbf{r}, t)|^2$  is the

EM energy stored in that mode, with  $n_T$  being the refractive index of the cavity at  $\omega_T$ , and assuming that all the radiated power at  $\omega_T$  is collected by means of a waveguide coupled evanescently to the cavity, one finds that a simple coupled-mode theory approach to this problem<sup>9</sup> yields the following expression for the power  $P_T$  emitted at  $\omega_T$

$$P_T = \left( \frac{4\pi c_0 n_T}{\varepsilon_0 \lambda_T^4} \right) \left( \frac{Q_T}{Q_{T,s}} \right) \left( \frac{Q_T}{\tilde{V}_T} \right) |a_1(t)|^2 |a_2(t)|^2 |\beta_{\text{eff}}|^2 \quad (1)$$

where  $Q_T$  and  $Q_{T,s}$  stand for the total quality factor and the external quality factor (i.e., the one governing the decay into the waveguide) of the resonator at  $\omega_T$ , respectively.  $\lambda_T$  denote the resonant wavelength corresponding to  $\omega_T$ , while  $\tilde{V}_T = V_T/(\lambda_T/n_T)^3$ , where  $V_T$  is the effective modal volume of the resonant mode at  $\omega_T$ .  $a_1(t)$  and  $a_2(t)$  are the modal amplitudes of the pump and idler electric fields inside the cavity (i.e., we define  $\mathbf{E}_{1,2}(\mathbf{r}, t) = a_{1,2}(t) \tilde{\mathbf{E}}_{1,2}(\mathbf{r})$ , where  $\tilde{\mathbf{E}}_{1,2}(\mathbf{r})$  represents the spatial mode profile inside the cavity at  $\omega_{1,2}$ , normalized so that  $|a_{1,2}(t)|^2$  is the EM energy stored in the cavity at the corresponding resonant frequency  $\omega_{1,2}$ ). Finally, the parameter  $\beta_{\text{eff}}$  governs the nonlinear coupling strength among the electromagnetic fields involved in the nonlinear difference-frequency mixing; essentially, it corresponds to the overlapping integral of the three electric fields involved in the considered nonlinear process (see Ref. 10 for details on this magnitude).

From Eq. (1), the enhancement of the power radiated by  $\mathbf{J}_T(\mathbf{r}, t)$  inside the cavity is apparent through the factor  $Q_T/\tilde{V}_T$ . If we now assume that, in addition to the confinement at the difference frequency  $\omega_T$ , the cavity is also designed to trap light at  $\omega_1$  and  $\omega_2$  (forming a triply-resonant system), another enhancement factor proportional to the product  $Q_1 Q_2$  (where  $Q_1$  and  $Q_2$  are the quality factors of the cavity at  $\omega_1$  and  $\omega_2$ , respectively) is introduced in the efficiency of the nonlinear conversion process, simply due to the recirculation of the pump and idler powers inside the cavity. Importantly, noticing that in this case  $|a_1(t)|^2 = (4Q_1/\omega_1)P_{1in}$  (where  $P_{1in}$  is the input power at  $\omega_1$ ), and that a similar expression holds for  $|a_2(t)|^2$ , from Eq.(1) one can show that (using realistic parameters, and keeping fixed the values of the pump power and area of interaction) the approach proposed in this work can introduce an enhancement factor for  $P_T$  as large as  $10^3$  with respect to the value of  $P_T$  one would obtain in a conventional difference-frequency generation process taking place, for instance, in a conventional phase-matched waveguide system.<sup>11</sup>

In order to explore the extent to which this concept could contribute to solve the current lack of efficient THz sources operating at room temperature, we illustrate its implementation in a specific structure based on a triply-resonant nonlinear configuration. Figure 1a displays a schematic of the proposed system. The power carried by two NIR beams of wavelengths  $\lambda_1$  and  $\lambda_2$  (playing the role of pump and idler beams, respectively, their corresponding power being  $P_{1in}$  and  $P_{2in}$ ) is coupled, by means of an index-guided waveguide, to two high-order whispering gallery modes (WGM) supported by a dielectric ring resonator. These WGM at  $\lambda_1$  and  $\lambda_2$  are characterized by angular momenta  $m_1$  and  $m_2$ , respectively. The ring resonator also acts as a dipole-like defect at  $\lambda_T$ , when embedded in an otherwise perfectly periodic THz-wavelength scale photonic crystal (PhC) formed by a square lattice of dielectric rods (see the

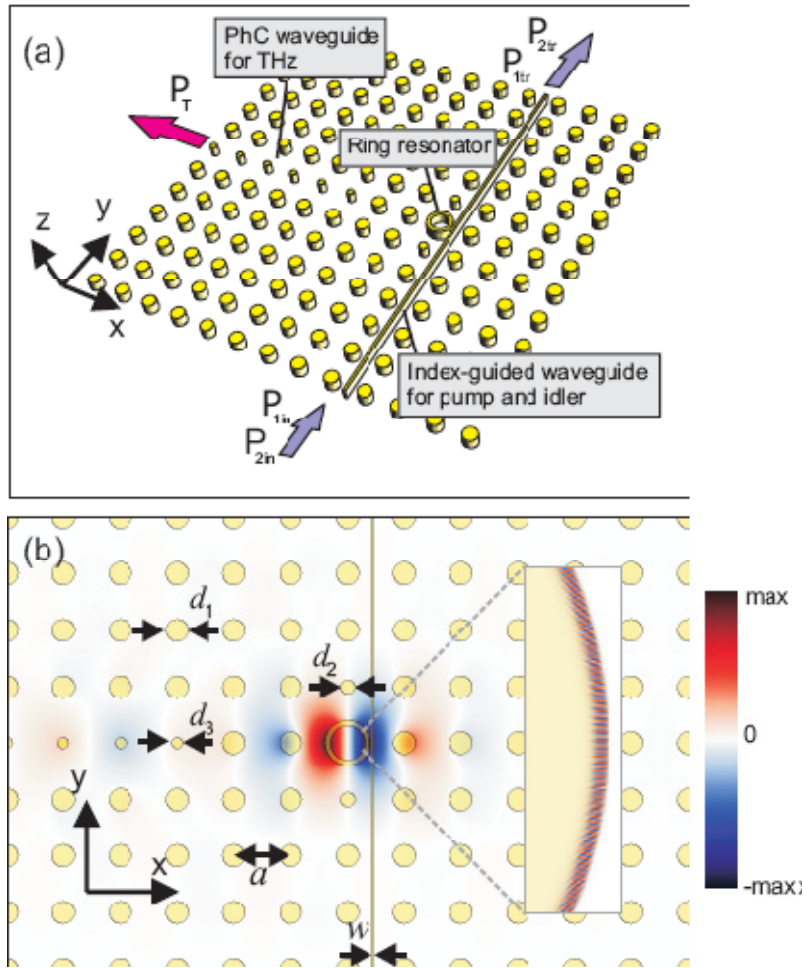


**Figure 1.** Schematic of the triply-resonant nonlinear photonic structure analyzed in the text.  $P_{in}$  and  $P_{2in}$  denote the input powers at the pump and idler frequencies, respectively; whereas  $P_{1tr}$  and  $P_{2tr}$  represent the corresponding transmitted powers through the structure.  $P_T$  stands for the THz output power. (b) Main panel: Electric field profile ( $E_z$ ) corresponding to the resonant mode appearing at 1THz in the structure shown in Fig. 1a. The value of the different geometrical parameters displayed in this figure are  $a=102 \mu\text{m}$ ,  $d_1=40.8 \mu\text{m}$ ,  $d_2=25.1 \mu\text{m}$ ,  $d_3=18.8 \mu\text{m}$ , and  $w=0.8 \mu\text{m}$ . Inset displays an enlarged view of the electric field profile ( $E_x$ ) corresponding to a whispering gallery with  $m=572$  circulating inside the dielectric ring shown in the main figure. The geometrical parameters defining the ring resonator are also shown in the inset,  $R_{ext}$  and  $R_{int}$  being  $40.1 \mu\text{m}$  and  $30.5 \mu\text{m}$ , respectively. Yellow areas in both the main and inset figures represent GaAs regions, while white areas represent air.

corresponding electric field profile in Fig. 1b). Thus, the  $\chi^{(2)}$  nonlinear frequency down-conversion interaction that takes place between the two NIR WGM's circulating inside the ring resonator yields a current distribution that radiates inside the PhC cavity at the frequency difference  $\omega_T = \omega_1 - \omega_2$ ; as mentioned, the rate at which the radiation is emitted is strongly enhanced by the PhC environment in which the ring resonator is embedded. In order to extract efficiently the THz output power ( $P_T$ ) from the PhC cavity, we introduce into the system a PhC waveguide created by reducing the radius of a row of rods (see Figs. 1a and 1b). In addition, in order to break the degeneracy existing between the  $x$ - and  $y$ -oriented dipole defect modes, and thus, further increase the efficiency of our approach, the radius of two of the nearest neighbors rods of the ring resonator is reduced with respect to the radius of other rods in

the PhC. The whole configuration permits having a large value for factor  $(Q_T/\tilde{V}_T)$ , along with a high- $Q$  resonant confinement also for the pump and idler frequencies.

Figure 1b shows the structure that results from optimizing the geometrical parameters of the system for efficient generation at 1 THz, along with the corresponding electric field profiles, as obtained from finite-difference time-domain (FDTD)<sup>12</sup> simulations. In these calculations we have assumed a pump beam of wavelength  $\lambda_1=1550\text{nm}$ , an idler beam with  $\lambda_2=1542\text{nm}$ , and that the structure is implemented in GaAs (in which the relevant component of the nonlinear susceptibility tensor is  $d_{14}=274\text{pm/V}$ [13]). For GaAs, and for the above cited values for  $\lambda_1$  and  $\lambda_2$ , we have found that the strength of the nonlinear coupling coefficient that governs the energy transfer between the pump, idler and THz fields is maximized if the structure is designed to support two WGM with  $m_1=572$  and  $m_2=575$  at  $\lambda_1$  and  $\lambda_2$ , respectively (see inset of Fig. 1b), and a dipole defect mode in the THz-scale PhC.

We emphasize that in conventional phase-matching schemes, the overall efficiency of a DFG process relies entirely on finding a suitable nonlinear material whose dispersion relation permits fulfilling simultaneously, for the frequency range of interest, both the frequency-matching and the phase-matching conditions<sup>6</sup> (or alternatively, on finding some physical mechanism, such as quasiphasematching, that permits matching of the different fields involved in the nonlinear process). However, in the approach introduced here, the dispersion relation corresponding to the final frequency  $\omega_T$  is different from that corresponding to  $\omega_1$  and  $\omega_2$  and, importantly, it can be tailored almost at will simply by modifying the

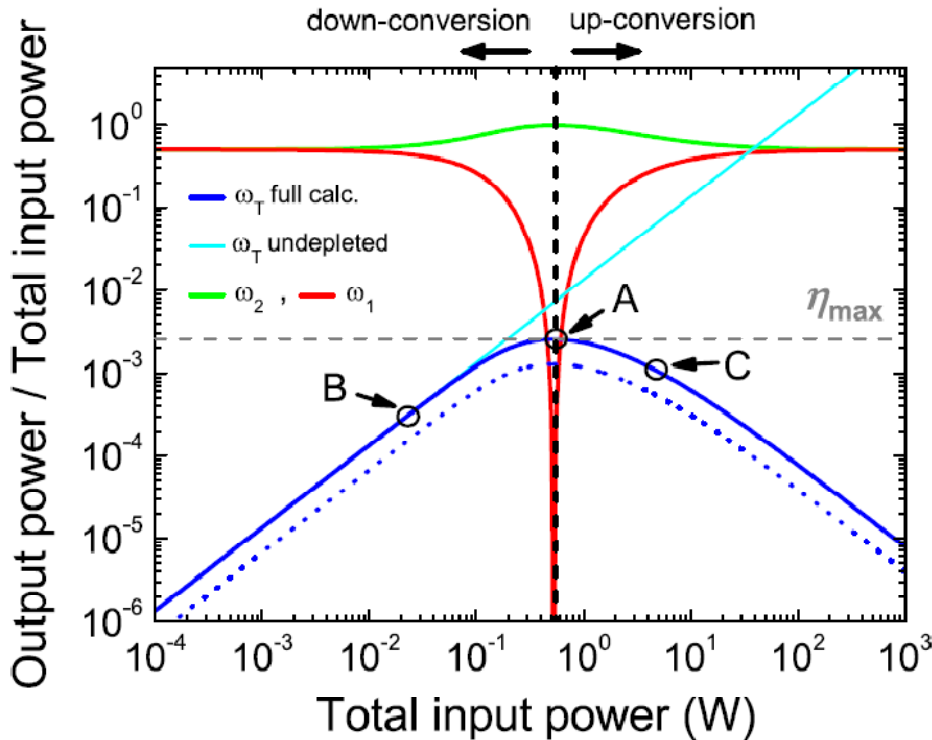


**Figure 2.** Ratio between the total output power emitted by the system at 1 THz and the total input power at the NIR pump and idler frequencies. The results for the three frequencies involved in the considered nonlinear down-conversion process are displayed ( $\omega_1$ ,  $\omega_2$ , and  $\omega_T$  correspond to the pump, idler, and final THz frequencies, respectively). Horizontal dashed line displays the maximum possible conversion efficiency  $\eta_{max}$  given by the Manley-Rowe quantum limit. Dotted line displays the effect of linear absorption losses on the conversion efficiency.

geometrical parameters that define the THz-scale PhC. This introduces a general and versatile route to phase-matching that does not depend exclusively on the intrinsic properties of naturally existing nonlinear optical materials, which could be particularly relevant in those systems in which the canonical phase-matching condition can not be fulfilled.

To compute accurately the nonlinear optical dynamics of the structure sketched in Fig. 1a, in both the undepleted and depleted regimes, we have applied a temporal coupled-mode theory (TCMT) [14] (see details in Refs. 15,10). Figure 2 summarizes the results obtained in the continuous-wave (cw) regime. In these calculations we have assumed that  $P_{1in} = P_{2in}$  and quality factors  $Q_1 = Q_2 = 3.5 \times 10^5$  and  $Q_T = 10^3$ . These values for  $Q$  are compatible with both the absorption coefficient of GaAs at 1 THz (the linear absorption rate of GaAs corresponds to a  $Q$  factor  $1.5 \times 10^3$ )<sup>16</sup> and the experimental values for the quality factors obtained in similar configurations for the considered ring resonator and also for the photonic crystal cavity.<sup>17,18</sup> As shown in Fig. 2, for values of the total input power ( $P_{tot,in} = P_{1in} + P_{2in}$ ) larger than 0.07W the conversion efficiency (defined here as ratio  $P_T/P_{tot,in}$ ) starts departing from the conversion efficiency predicted by the undepleted approximation, eventually reaching the maximum value predicted by the Manley-Rowe relation.<sup>6</sup> As clearly shown in Fig. 2, at the critical value of the total input power at which this maximum conversion efficiency is reached ( $P_{tot,in}^c = 0.54W$ ) the pump power that is coupled to the ring resonator is completely down-converted inside the system to power at THz and idler frequencies, giving rise to a sharp minimum in  $P_{1tr}$  and a maximum in  $P_{2tr}$ . This represents a dramatic reduction in  $P_{tot,in}$  with respect to the most efficient schemes for THz generation in nonlinear crystals reported up to date.<sup>2,3</sup> Furthermore, we emphasize that, in addition to powerful lasers, current efficient schemes for THz generation require intricate phase-matching set-ups, whereas in the system introduced in this manuscript the maximum theoretically possible efficiency can be achieved in an integrated structure having a total area of approximately  $1\text{mm}^2$  and using  $<1W$  power levels, which are readily accesible with compact turn-key sources. Note that since  $P_0 \propto 1/Q_1Q_2Q_T$ , the value of  $P_{tot,in}^c$  can be adjusted just by varying the product  $Q_1Q_2Q_T$ . We also point out that the net effect of the absorption losses in the conversion efficiency consists simply in downscaling the results obtained in the lossless case by a factor  $Q_T/Q_{T,s}$  (see dotted line in Fig. 2).

In order to completely characterize the THz generation process in the analyzed structure we have also studied the temporal evolution of the response of the system to Gaussian pulse excitations. In these calculations we assume that the temporal width of the pulses  $\tau_{THz}$  is larger lifetime of the THz-scale cavity (we have chosen  $\tau_{THz} = 32\text{ns}$ ). The value of  $\tau_{THz}$  is much larger than the lifetime of the WGM modes at the pump and idler frequencies ( $\approx 0.6\text{ns}$ ). Thus, we expect similar conversion maximum efficiencies as those found in the cw analysis described above. Figures 3a-c show the results corresponding to three representative values for the peak power of  $P_{1in}(t)$  (labeled as A,B and C, respectively, in Fig. 2b), while Fig. 3d displays a summary of our time-dependent simulations in terms of the ratio between the output THz energy and total input NIR energy (defined as  $E_{THz} = \int_0^\infty dt P_T(t)$ , and  $E_{NIR} = \int_0^\infty dt [P_{1in}(t) + P_{2in}(t)]$ , respectively). As displayed in Fig. 3d, the maximum conversion efficiency can be reached for an input energy  $E_{NIR} = 0.02 \mu\text{J}$ .

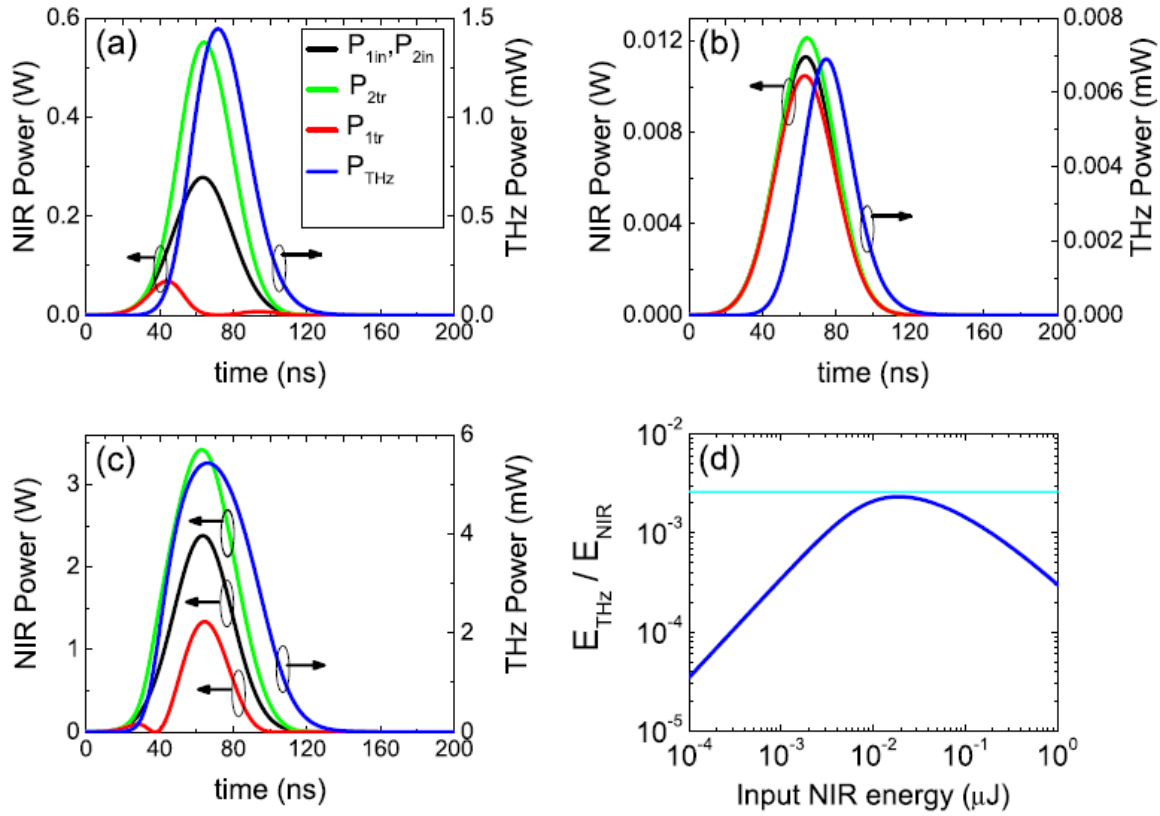


**Figure 3.** Analysis of the temporal response of the system shown in Fig. 1a to gaussian excitation pulses. Panels a, b, and c correspond to the peak values for  $P_{in}$  shown by labels A,B, and C, respectively in Fig. 2. Panel d displays the ratio between the total output energy ( $E_{THz}$ ) and the total NIR input energy ( $E_{NIR}$ ) as a function of  $E_{NIR}$ . Horizontal line in panel d corresponds to the maximum possible conversion efficiency predicted by the Manley-Rowe quantum limit.

In conclusion, we have shown the dramatic enhancement of the conversion efficiency of general difference-frequency downconversion processes enabled by triply-resonant photonic resonators. By means of detailed numerical simulations, we have illustrated the relevance of the proposed scheme by demonstrating that in the continuous-wave regime the pump powers required to reach quantum-limited conversion efficiency can be reduced dramatically with respect to the conventional approaches for THz generation employed up to date. We believe these results could enable a broader use of THz sources.

### Acknowledgements

The authors thank Dr. Morris Kesler and Dr. Katie Hall for valuable discussions. This work was supported by the MRSEC Program of the NSF under award number DMR-0819762 and by the U.S.A.R.O. through the ISN under Contract No. W911NF-07-D-0004.

## References

- <sup>1</sup> M. Tonouchi, *Nature Phot.* **1**, 97 (2007).
- <sup>2</sup> K. L. Vodopyanov, M. M. Fejer, X. Yu, J. S. Harris, Y.-S. Lee, W. C. Hurlbut, V. G. Kozlov, D. Bliss, and C. Lynch, *Appl. Phys. Lett.* **89**, 141119 (2006).
- <sup>3</sup> K.-L. Yeh, M.C. Hoffmann, J. Hebling, and K.A. Nelson, *Appl. Phys. Lett.* **90**, 171121 (2007).
- <sup>4</sup> Y. A. Morozov, I. S. Nefedov, V. Y. Aleshkin, and I. V. Krasnikova, *Semiconductors* **39**, 113 (2005).
- <sup>5</sup> Z. Ruan, G. Veronis, K. L. Vodopyanov, M. M. Fejer, and S. Fan, *Opt. Express* **17**, 13502 (2009).
- <sup>6</sup> R. W. Boyd, *Nonlinear Optics*, 2nd ed. (Academic Press, San Diego, 2003).
- <sup>7</sup> E. U. Condon, *J. Appl. Phys.* **12**, 129 (1941).
- <sup>8</sup> E. Purcell, *Phys. Rev.* **69**, 681 (1946); Y. Xu, R.K. Lee, A. Yariv, *Phys. Rev. A* **61**, 033807 (2000).
- <sup>9</sup> H. A. Haus, *Waves and Fields in Optoelectronics* (Prentice-Hall, Englewood Cliffs, NJ, 1984).
- <sup>10</sup> I.B. Burgess, A.W. Rodriguez, M.W. McCutcheon, J. Bravo-Abad, Y. Zhang, S.G. Johnson, M. Loncar, *Opt. Express* **17**, 9241 (2009).
- <sup>11</sup> V.G. Dmitriev, G.G. Gurzadyan, and D.N. Nikogosyan, *Handbook of Nonlinear Optical Crystals* (Springer, New York, 1991).
- <sup>12</sup> A. Taflove and S. C. Hagness, *Computational Electrodynamics: The Finite-Difference Time-Domain Method*, 3rd ed. (Artech, Norwood, 2005).
- <sup>13</sup> S. Singh, *Nonlinear Optical Materials* in M.J. Weber Ed., *Handbook of laser science and technology*, Vol. III: Optical Materials, Part I, (CRC Press, 1986).
- <sup>14</sup> Due to the vast difference between the wavelength corresponding to the pump and final THz frequency, standard numerical methods used in nonlinear nanophotonics (such as the nonlinear FDTD) are not suitable for this problem.
- <sup>15</sup> H. Hashemi, A.W. Rodriguez, J.D. Joannopoulos, M. Soljacic, and S. G. Johnson, *Phys. Rev. A* **79**, 013812 (2009).
- <sup>16</sup> J. Hebling, A.G. Stepanov, G. Almasi, B. Bartal, and J. Kuhl, *Appl. Phys. B* **78**, 593 (2004).
- <sup>17</sup> S. Noda, M. Fujita, and T. Asano, *Nature Phot.* **1**, 449 (2007).
- <sup>18</sup> V. R. Almeida, C. A. Barrios, R.R. Panepucci, M. Lipson, *Nature* **431**, 1081 (2004).



## Publications

### Journal Articles Published

"Efficient low-power terahertz generation via on-chip triply-resonant nonlinear frequency mixing" Jorge Bravo-Abad, Alejandro W. Rodriguez, J. D. Joannopoulos, Peter T. Rakich, Steven G. Johnson, and Marin Soljagic. *Appl. Phys. Lett.* **96**, 101110, (2010).

"Light scattering from anisotropic particles: propagation, localization, and nonlinearity" Chengwei Qiu, Lei Gao, John D. Joannopoulos, and Marin Soljagic. *Laser & Photonics Reviews* **4**, No.2, p.268, (2010).

"Simultaneous mid-range power transfer to multiple devices" Andre Kurs, Robert Moffatt, and Marin Soljagic. *Appl. Phys. Lett.* **96**, 044102, (2010).

"Plasmonics in graphene at infrared frequencies" Marinko Jablan, Hrvoje Buljan, and Marin Soljagic. *Phys. Rev. B* **80**, 245435, (2009). Also appeared as an *Invited Paper in Virtual Journal of Nanoscale Science and Technology* January 2010.

"Observation of unidirectional backscattering-immune topological electromagnetic states" Zheng Wang, Yidong Chong, J.D.Joannopoulos, and Marin Soljagic. *Nature* **461**, p.772, (2009).

"Plasmonic-Dielectric Systems for High-Order Dispersionless Slow or Stopped Subwavelength Light" Aristeidis Karalis, J.D.Joannopoulos, and Marin Soljagic. *Phys. Rev. Lett.* **103**, 043906, (2009). Also appeared as an *Invited Paper in Virtual Journal of Nanoscale Science and Technology* July 2009.

"Ultrafast photodetection in an all-silicon chip enabled by two-photon absorption" J. Bravo-Abad, E. P. Ippen, and Marin Soljagic. *Appl. Phys. Lett.* **94**, 241103, (2009). Also appeared as an *Invited Paper in Virtual Journal of Ultrafast Science* July 2009.

"Efficient weakly-radiative wireless energy transfer: An EIT-like approach" Rafif E. Hamam, Aristeidis Karalis, J.D. Joannopoulos, and Marin Soljagic. *Annals of Physics* **324**, 1783, (2009).

### PhD theses

Rafif Hamam, Thesis (PhD), "Novel Resonant and Light-Guiding Phenomena in Photonics", Massachusetts Institute of Technology, Dept. of Physics, 2010.

Alejandro Rodriguez, Thesis (PhD), "Nonlinear nanophotonics and fluctuation-induced interactions", Massachusetts Institute of Technology, Dept. of Physics, 2010.

Michael Ghebrebrhan, Thesis (PhD), "Anomalous phenomena and spectral tailoring in photonic crystals", Massachusetts Institute of Technology, Dept. of Physics, 2010.